Available online at www.sciencedirect.com

SciVerse ScienceDirect

Procedia IUTAM 8 (2013) 144 – 152

Procedia IUTAM

www.elsevier.com/locate/procedia

IUTAM Symposium on Waves in Fluids: Effects of Nonlinearity, Rotation, Stratification and Dissipation

The Effect of Viscoelasticity on Breaking Standing Waves

Vladimir A. Kalinichenko [a]*, Somchai Wongwises [b]

[a] *A.Ishlinsky Institute for Problems in Mechanics RAS, Moscow Russia*
[b] *King Mongkut's University of Technology Thonburi, Bangkok Thailand*

Abstract

Here we present novel experimental evidence that the presence of polymer in water dramatically affects the transition to breaking standing gravity surface waves excited under Faraday resonance. Our measurements showed that by adding of a small amount of polymers to the distilled water the transition into wave breaking state was delayed, and the elongational viscosity of the polymer solution accounts for this behavior.

Keywords: gravity surface Faraday waves; parametric resonance, wave breaking; polymer solution; elongational viscosity.

1. Inroduction

Relating to the class of free surface problems the steep and breaking water waves are of interest to fundamental hydrodynamics [1 – 3] as well as engineering applications [4, 5]. The formation of vertical jets, splashes and plumes of water frequently accompany the impact of progressive waves against a vertical wall. Other examples of such behavior are known to occur in standing gravity waves in cylindrical [6] and rectangular [7] tanks when a jet arises out of a wave antinode. The formation of these jets can be referred to a class of nonstationary problems of the cavity collapse on a free surface of a liquid; these problems were always of great interest to researchers because of high-speed cumulative jet generation and of its subsequent fragmentation. As theoretical modeling of the given phenomenon is completed by localized surface singularities, the laboratory experiment on the dynamics of collapsing cavity takes on special significance.

The object of our experimental study is breaking standing gravity waves excited by the parametric resonance. Since Faraday's founding work [8], much is already known about the excitation of these Faraday waves and their limit characteristics. So far, the breaking waves have been mostly studied in simple Newtonian viscous fluids [7, 9, 10]. Recently, interest has grown in the effect of vertical vibrations on a layer of complex non-Newtonian

* Corresponding author. Tel.: +7-495-434-1487; fax: +7-499-739-9531.
E-mail address: kalin@ipmnet.ru

doi:10.1016/j.piutam.2013.04.018

fluids, e.g. [11 – 13]. Due to their microstructure, complex fluids display viscoelastic properties, which may affect classical hydrodynamic instabilities. Previous experiments showed the significant effect of diluted flexible polymers on a parametrically driven, disordered capillary waves [12, 13].

In this paper, we report novel experimental evidence that polymers affect the transition to breaking standing gravity surface waves excited under Faraday resonance.

2. Experimental procedure

Experiments were performed with an electromechanical shaking table (Fig. 1(a)) with a frequency range of 0.3 - 10 Hz. The second wave mode ($n = 2$) was excited under the conditions of main Faraday resonance ($\Omega \sim 2\omega$) in a rectangular acrylic tank ($50 \times 4 \times 40$ cm) which was filled with liquid to a depth of $h = 15$cm and oscillated vertically with amplitude s =0.75 cm and frequency Ω . At the fixed value of s the variation of Ω provided change of a wave steepness $\Gamma = H / \lambda$ (H is the wave height, $\lambda = 50$cm is the wavelength, $\omega^2 = gk \operatorname{th} kh$, $k = 2\pi / \lambda$). Waves produced in this way could be precisely controlled under experimental conditions [14]. The wave profiles were obtained by the use of regular (DIMAGE Z2, 30 fps) and high-speed (VS FAST, 200-500 fps) video cameras oscillating with the tank, and image processing by the software ImageJ 1.43u†. The behavior of surface waves was examined by slowly increasing or decreasing Ω , with s fixed. In order to exclude transient effects, we made the observation and recording of surface waves after waiting for at least 200 - 300 forcing periods, keeping Ω fixed.

Aqueous solutions of polyacrilamide (PAM) with molecular mass $M = 11 \times 10^6$ g/mol at concentrations $C = 10, 100, 500, 1000$ ppm were used in this work. The wave breaking processes in pure water ($C = 0$) is treated as a "reference point". Most of our experiments were conducted with water and PAM solutions, but to estimate the viscous effect we also used aqueous solution of sugar (density: 1.236 g/cm^3; kinematic viscosity: 13.43 cSt).

3. Breaking Faraday waves

3.1. The collapsing cavity

Since the linear stability of Faraday waves [15] is described by the dimensionless detuning parameter $p = \left(2\omega / \Omega\right)^2$ and the forcing parameter $q = 2\kappa s \tanh \kappa h$, the parametric excitation of waves can be interpreted in the (*p, q*)-plane. The neutral stability chart (Fig. 1(b), the plot in the upper right corner) determines the (*p, q*)-values corresponding to the condition of subharmonic resonance from quiescent initial fluid states, i.e. the unstable region in (*p, q*)-plane. Consequently, each regime of fluid oscillations in our experiments can be quantitatively represented by pair values of (*p, q*). This approach has special value in case of irregular and breaking waves since their height *H* can be estimated only in statistical sense.

The observable Faraday waves can be separated into three classes – regular, irregular and breaking waves. Locations of these waveforms in (*p, q*) parameter space are shown in Fig. 1(b). Regular waves (region 1) are periodic and symmetric in time and space. It was determined [9] that they have a limit steepness of 0.255, and a limiting angle at a crest less than 80°. For irregular waves (region 2), the temporal and space symmetry is broken. Observe that in regular and irregular waves, the volume of the oscillating liquid keeps its connectivity. Breaking Faraday waves (region 3) occupying the most part of (*p, q*)-plane are characterized by the broken free liquid surface with ejected drops and jets.

---

†Freely distributed on the Internet: http://rsbweb.nih.gov/ij/. No license is required

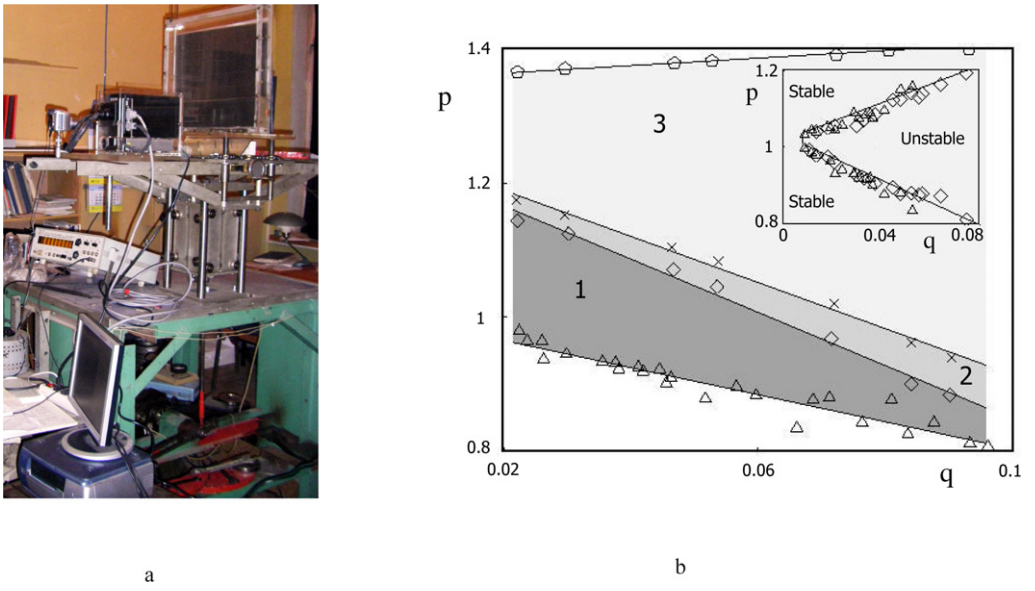

Fig. 1. (a) The experimental setup. (b) Locations of the various waveforms in parametric space (p, q): 1 – regular; 2 – irregular; 3 – breaking waves. Shaded areas determine the approximate boundaries of waveforms. The plot in the upper right corner of this figure is the stability chart of the free surface of the liquid for second and third wave modes (n =2, 3)

Careful analysis of the high-speed video data shows that the wave breaking process occurs in the following scenario of jet generation in sharp-crested wave mode. The origin of the jet is due to the cavity collapsing at the crest formation stage when the central part of the fluid moves upward - Fig. 2(a). When a cavity on the wave crest collapses, it generally produces a well-defined high velocity jet.

As shown in Fig. 2(a), during the crest formation from the initial "horizontal" free surface position, the first observable cavity is a shallow depression with an almost flat bottom (frame 2); the length of this deepening (from edge to edge) is about 8 cm. For the description of the cavity dynamics, we use its length l and depth d measured with respect to the free surface of the liquid. The length of the first observable cavity is considered as the initial value of l_0. From the moment of cavity occurrence, its length monotonously decreases (frames 2-9). However the cavity depth first reaches the maximum, d_0~1.1 cm (frame 4), and then decreases to zero at the moment of cavity closure. Hence, from the moment of the maximal depth d_0, the cavity stops growing downward and the process of its collapse begins. This means that the vertical velocity of the liquid around the cavity bottom has reached a zero value and has changed its sign. Taking into account the monotone length change, this is evidence of complex flow pattern near the cavity boundaries. Note that at the maximal depth d_0, the cavity takes the shape of a semicylinder. After cavity closure has occurred (frame 10, time t_0 = 0.1 s), a jet of liquid forms at the point of closure and moves together with the growing wave crest (frames 11-14). Finally, the jet breaks down into liquid fragments (frames 15-21). Hence, the entire collapsing process taking place within about 40 - 70 ms can be divided into two stages: 1) the cavity is initiated and grows on the forming crest above the still water level, and 2) it collapses.

The detailed analysis of the process of the cavity collapsing in Fig. 2(b) shows that in 0.01 s after the moment when d_0 = 1.3 cm (frame 1), the cavity takes the dihedral form (frame 3) with a linear angle of about 112°. Then the bottom of the dihedral surface is rounded (frame 4), and until the cavity closure (frames 5 and 6), any jets are absent. The initial indication of jet ejection can be only noted in frames 7 – 8.

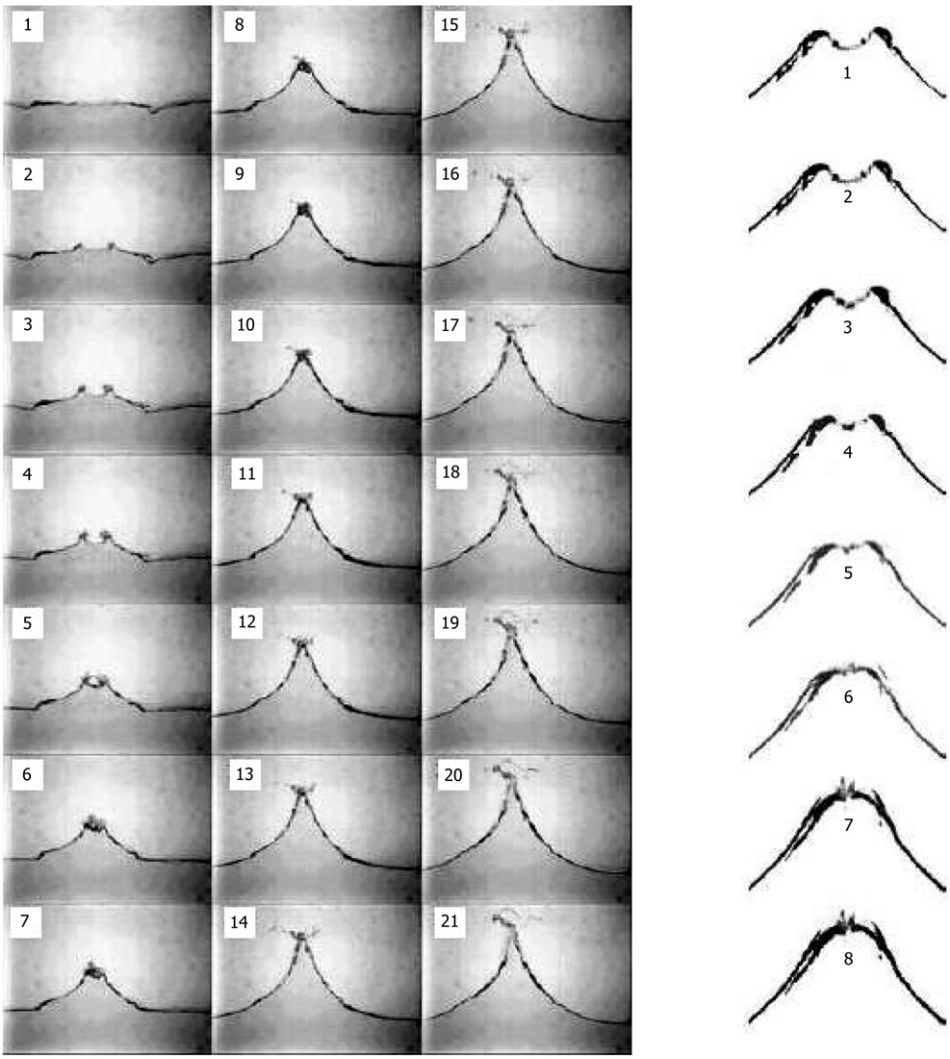

a b

Fig. 2. Sequence of video frames showing details of breaking Faraday waves. The numbers superposed on the images determine their sequence order. (a) Initiation, development and collapse of the cavity during crest formation; $p = 1.109$, $q = 0.180$. (b) Cavity collapse on forming crest; $p = 0.941$, $q = 0.180$; the maximal depth of a cavity is $d_0 = 1.3$ cm; the field of view is 5×5 cm. The images are taken at time intervals 0.01s (a), and 0.005s (b), respectively

The sequence of events presented in Fig. 2 and described above is general for breaking Faraday waves on a free surface of water, aqueous solutions of sugar and PAM in a rectangular tank. The initiation, development and collapsing of the cavity takes place during wave crest forming after the free surface has passed the still water level. It is necessary to note basic difference of this our conclusion from all previous experiments, e.g. [16], in which the jet eruption in axisymmetric standing waves on the free surface of liquids in cylindrical tanks was considered. All authors observed the translation of the rising trough (below the still water level) to a narrow jet. Numerical model [17] also considered formation of a jet from a trough of a standing wave in a rectangular tank.

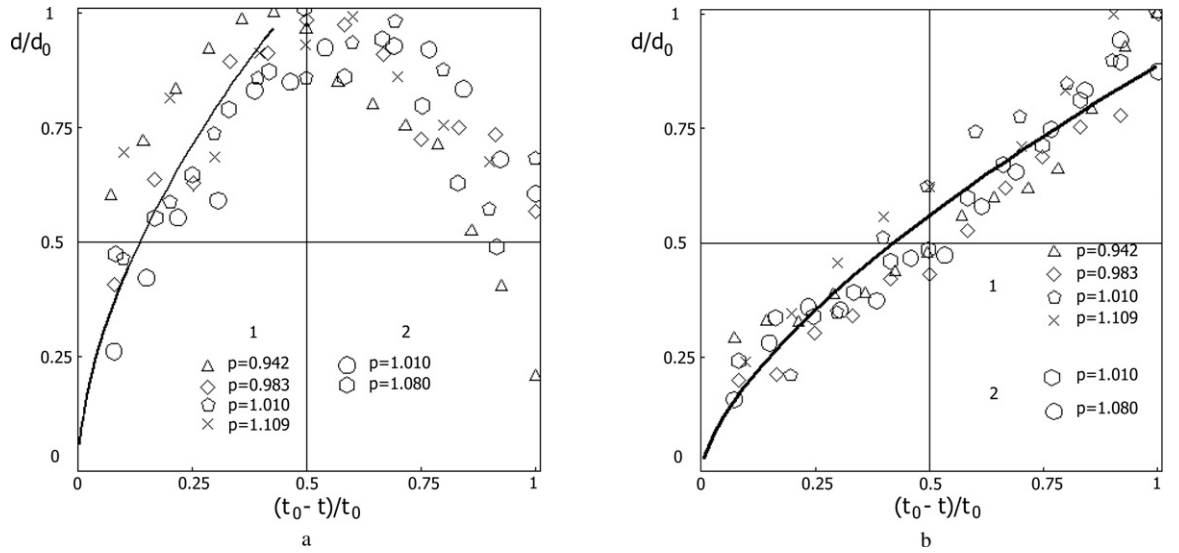

Fig. 3. Cavity depth (a) and length (b) at various times after cavity formation $(t_0 - t)/t_0 = 1$ and before cavity collapse $(t_0 - t)/t_0 = 0$; q = 0.090, p = 0.942, 0.983, 1.010, 1.109 and 1.080. Experimental points 1 and 2 correspond to water and aqueous solution of sugar (density: 1.236 g/cm^3; kinematic viscosity: 13.43 cSt), respectively. The solid line is the functional dependency $(1 - t/t_0)^{-2/3}$ for dimensionless geometrics of collapsing cavity

Dimensionless dependencies of cavity depth d/d_0 and length l/l_0 from time $(t_0 - t)/t_0$ are presented in Fig. 3, where t_0 is the time of cavity closure. All the data for water and aqueous solution of sugar collapse reasonably well into a single curve at the stage of cavity collapse:

$$(l/l_0; d/d_0) \sim \left(1 - t/t_o\right)^{2/3}$$

This relationship reflects a monotonic decrease in cavity length and depth with increasing time. Solid lines on Fig. 3 correspond to functional dependency $\left(1 - t/t_o\right)^{2/3}$. It is significant that the $2/3$ - exponent reflects the general laws inherent in problems [18,19] with a conic deepening on a free surface of a liquid and most likely corresponds to a balance between inertia and surface tension. It seems that the viscosity effects are small in our case (*see* Fig. 3, data for water and aqueous sugar solution) and do not exert influence on process of a cavity collapse.

Using the data on cavity dynamics, we estimate the velocities of the fluid particles in pure wave motion and in the collapsing cavity. The maximum wave velocity (horizontal or vertical) of the free surface particles is about 90 cm/s. The average horizontal and vertical closure velocities have the same order of value (~ 50 – 150 cm/s). However, at the moment of cavity closure, there was a velocity jump (~ 400 cm/s), and the corresponding estimation for vertical acceleration gives a value of about 30 – 40g.

3.2. Ejected jets and the effect of viscoelasticity

Experiments showed almost no difference between Newtonian and non-Newtonian fluids for regular and irregular Faraday waves. Resonance curves $H(\Omega)$ in Fig. 4 show that with decrease in the tank frequency Ω the height of regular and irregular waves monotonically increases without significant differences between water and polymer solutions.

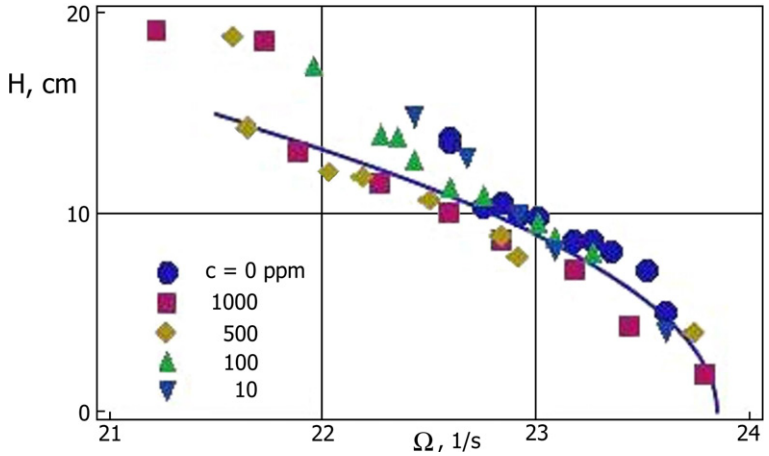

Fig. 4. Resonance curves of non-breaking waves on free surface of water and polymer solutions

The transition to wave-breaking state occurs at a further frequency decreasing. For water, this state means a change from a simply connected surface to a free surface connected in multiple ways. At close examination the formation of the ejected jet is associated with the collapsing cavity during crest formation when the central part of fluid moves upward. When a cavity of the developing wave crest collapses, it generally produces a well-defined high velocity jet.

Figure 5 shows two typical images of the jet evolution for pure water (a), and for PAM aqueous solution, $C = 10^3$ ppm (b). In these pictures, the images were obtained using the same driving frequency $\Omega = 20.81$ s^{-1}. It can be seen that the presence of a small polymer concentration fundamentally changes the structures of the ejected jet.

In both cases, the ejected jet is stretched due to the difference of the growing crest velocity and cumulative velocity of the jet tip. This difference is estimated to be about 150 – 200 cm/s.

A water stretched jet on the growing crest breaks into droplets, which can be clearly seen from 35 ms and on - Fig. 5(a).

The picture changes drastically in the case of polymer solutions – Fig. 5(b). The stretched jet keeps its integrity practically for the entire time interval (320 ms). One can see only a single drop when the wave surface moves to the undisturbed horizontal level (downward motion of the free surface).

The main morphological differences between the stretched jets of water and PAM solution are explained from a molecular standpoint. The presence of PAM molecules increases the elongational viscosity of the fluid [20]. The retardation of breakup of polymeric liquids may be attributable to the fact that in the process of disintegration the liquid is subjected to strong local tensile deformation along the jet. At the same time, one of the most unusual properties of polymeric liquids is the ability to accumulate giant reversible strains and develop high elastic stresses in strong elongational flows. Formally, this corresponds to multiple increase in the longitudinal (elongational) viscosity. In liquid disintegration the elastic stresses impede the separation of the liquid continuum into isolated fragments

The effect of polymer additives is particularly evident in the construction of the free surface envelope built upon overlapping of wave profiles for several wave periods – Fig. 6.

To quantify the effect of polymer additives we used the steepness of waves without droplet detachments. The corresponding dependence $\Gamma(C)$ is shown in Fig. 7.

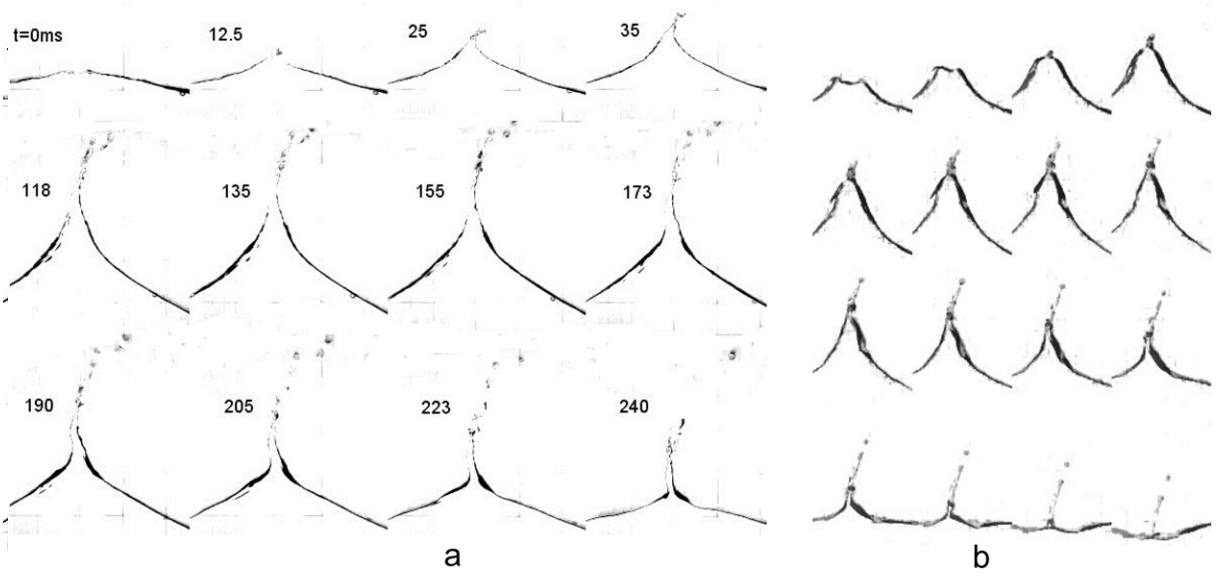

Fig. 5. Comparative evolution of the ejected jets for: a – a pure water; b – PAM ($C = 10^3$ ppm; time step between frames Δt =20 ms). Driving frequency $\Omega = 20.81$ s^{-1}

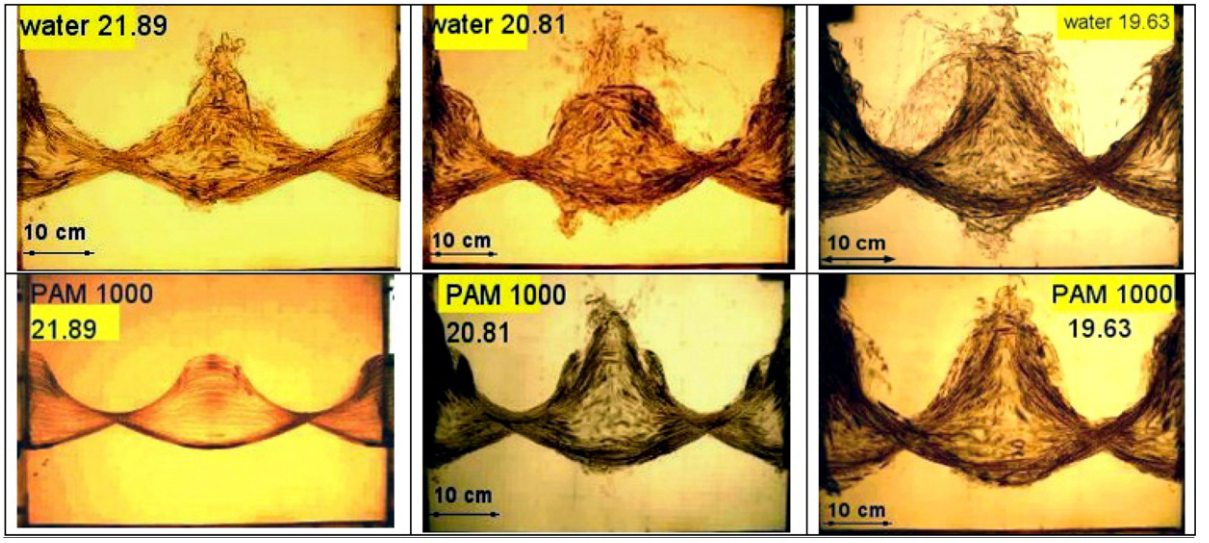

Fig. 6. . Development (water – top row of pictures) and suppression (PAM, $C = 10^3$ ppm – bottom row of pictures) of liquid spray formation over the upper wave envelopes at $\Omega = 21.89$, 20.81 and 19.63 s^{-1}. The envelopes have obtained by overlapping the wave profiles for 15 wave periods with a time step of 1/30 s

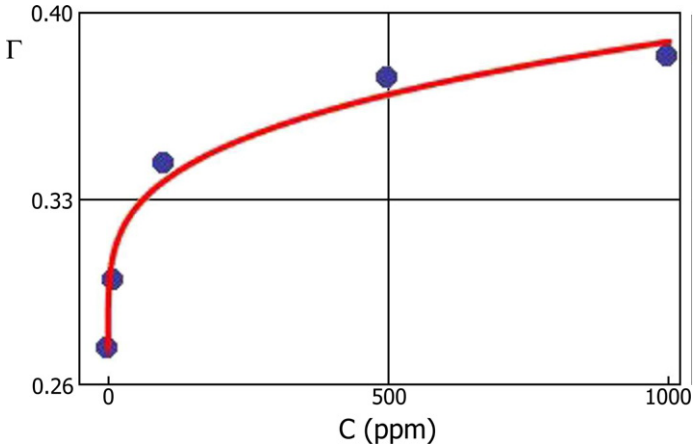

Fig. 7. The dependence of the steepness of waves without liquid fragmentation on the concentration of polymer

Thus, in pure water the ejected jets break up into droplets due to Rayleigh instability – there is a tendency towards the development of beadlike swellings and contractions along the jet. These swellings and contractions (initially small in size) grow until ultimately the jet is broken into drops (Fig. 5(b)). In the polymer solution the long and stable filament-like peak is visible (Fig. 5(b)). In fact, such peaks prevent from liquid spray formation over upper wave envelopes (Fig. 6). As a result, the steepness of Faraday waves in non-Newtonian liquids increases significantly (Fig. 7).

4. Concluding remarks

We have presented novel experimental results on breaking standing gravity waves in viscoelastic liquids. We obtain a significant strengthening effect of the oscillating liquid at polymer (PAM) concentrations of about 10 - 1000 ppm.

Without PAM additives we observed a rapid development of Rayleigh instability along the jet ejected from the growing wave crest and the subsequent fragmentation of this jet into drops.

The addition of the polymer possessing elastic properties suppress the jet breakup which significantly increases of the steepness of non-breaking Faraday waves.

Acknowledgements

Experiments were performed at the “PR-2M” USU setup “HPC IPMech RAS” (State contract 16.518.11.7059) with the partial support of the Thai Research Fund and the Commission on Higher Education of Thailand, and the Russian Foundation for Basic Research (Pr. No. 12-08-00067).

References

[1] Whitham GB. *Linear and nonlinear waves.* New York: Wiley-Interscience; 1974.
[2] Penney WG, Price AT. Finite periodic stationary gravity waves in a perfect fluid. *Phil. Trans. Roy. Soc. Lond.* 1952;**A224**:254 – 84.
[3] Taylor GI. An experimental study of standing waves. *Proc. Roy. Soc. Lond.* 1953;**A218**:44 – 59.
[4] Ibrahim RA. *Liquid sloshing dynamics: theory and applications.* Cambridge: University Press; 2005.
[5] Peregrine DH. Water-wave impact on walls. *Ann. Rev. Fluid Mech.* 2003;**35**:23 – 43.

[6] Longuet-Higgins MS. Bubbles, breaking waves and hyperbolic jets at a free surface. *J. Fluid Mech.* 1983;**127**:103 – 21.
[7] Jiang L, Ting CL, Perlin M, Schultz WW. Moderate and steep Faraday waves: instabilities, modulation and temporal asymmetries. *J. Fluid Mech.* 1996;**329:**215 – 307.
[8] Faraday M. On a peculiar class of acoustical figures, and on certain forms assumed by groups of particles upon vibrating elastic surfaces. *Phil. Trans. Roy. Soc. Lond.* 1831;**121**:299 – 340.
[9] Kalinichenko VA, Sekerzh-Zenkovich SYa. An experimental study on maximal height Faraday waves. *Fluid Dynamics* 2007;**42**:959 – 65.
[10] Kalinichenko VA. Breaking Faraday waves and jet launch formation. *Fluid Dynamics* 2009;**44**:577 – 86.
[11] Ballesta P, Manneville S. Signature of elasticity in the Faraday waves. *Phys.Rev.E* 2005;**71**:026308.
[12] Kityk AV, Wagner C. Delay of disorder by diluted polymers. *EPL* 2006;**75**(3):441 – 7.
[13] Shats M, Xia H, Punzmann H. Parametrically excited water surface ripples as ensembles of oscillons. *PRL* 2012;**108**:034502.
[14]. Kalinichenko VA, Nesterov SV, Sekerzh-Zen'kovich SYa, Chaykovskii AA. Experimental study of surface waves with Faraday resonance excitation. *Fluid Dynamics* 1995;**30**:101 – 6.
[15] Benjamin TB, Ursell F. The stability of the plane free surface of a liquid in vertical periodic motion. *Proc.R.Soc.Lond.* 1954;**A225**:505 – 15.
[16] Zeff BW, Kleber B, Fineberg J, Lathrop DP. Singularity dynamics in curvature collapse and jet eruption on a fluid surface. *Nature* 2000;**403**:401 – 4.
[17] Longuet-Higgins MS, Dommermuth DG. Vertical jets from standing waves. II *Proc.R.Soc.Lond.* 2001;**A457**:2137 – 49.
[18] Duchemin L, Popinet S, Josserand C, Zaleski S. Jet formation in bubbles bursting at a free surface. *Phys. Fluids* 2002;**14**:3000 – 8.
[19] Eggers J, Fontelos M, Leppinen AD, Snoeijer JH. Theory of the collapsing axisymmetric cavity. *Phys. Rev. Lett.* 2007;**98**:094502.
[20] Rozhkov AN. Dynamics and breaking of viscoelastic liquids (a review). *Fluid Dynamics* 2005;**40**:835 – 53.